

**This is an electronic reprint of the original article.
This reprint *may differ* from the original in pagination and typographic detail.**

Author(s): Ośmiałowski, Borys; Zakrzewska, Anna; Jędrzejewska, Beata; Grabarz, Anna; Zaleśny, Robert; Bartkowiak, Wojciech; Kolehmainen, Erkki

Title: Influence of Substituent and Benzoannulation on Photophysical Properties of 1-Benzoylmethyleneisoquinoline Difluoroborates

Year: 2015

Version:

Please cite the original version:

Ośmiałowski, B., Zakrzewska, A., Jędrzejewska, B., Grabarz, A., Zaleśny, R., Bartkowiak, W., & Kolehmainen, E. (2015). Influence of Substituent and Benzoannulation on Photophysical Properties of 1-Benzoylmethyleneisoquinoline Difluoroborates. *Journal of Organic Chemistry*, 80(4), 2072-2080.
<https://doi.org/10.1021/jo502244j>

All material supplied via JYX is protected by copyright and other intellectual property rights, and duplication or sale of all or part of any of the repository collections is not permitted, except that material may be duplicated by you for your research use or educational purposes in electronic or print form. You must obtain permission for any other use. Electronic or print copies may not be offered, whether for sale or otherwise to anyone who is not an authorised user.

Article

The influence of substituent and benzoannulation on photophysical properties of 1-benzoylmethyleneisoquinoline difluoroborates

Borys Osmialowski, Anna Zakrzewska, Beata Jedrzejewska, Anna Maria Grabarz, Robert Zalesny, Wojciech Bartkowiak, and Erkki Kolehmainen

J. Org. Chem., **Just Accepted Manuscript** • DOI: 10.1021/jo502244j • Publication Date (Web): 29 Jan 2015

Downloaded from <http://pubs.acs.org> on February 3, 2015

Just Accepted

“Just Accepted” manuscripts have been peer-reviewed and accepted for publication. They are posted online prior to technical editing, formatting for publication and author proofing. The American Chemical Society provides “Just Accepted” as a free service to the research community to expedite the dissemination of scientific material as soon as possible after acceptance. “Just Accepted” manuscripts appear in full in PDF format accompanied by an HTML abstract. “Just Accepted” manuscripts have been fully peer reviewed, but should not be considered the official version of record. They are accessible to all readers and citable by the Digital Object Identifier (DOI®). “Just Accepted” is an optional service offered to authors. Therefore, the “Just Accepted” Web site may not include all articles that will be published in the journal. After a manuscript is technically edited and formatted, it will be removed from the “Just Accepted” Web site and published as an ASAP article. Note that technical editing may introduce minor changes to the manuscript text and/or graphics which could affect content, and all legal disclaimers and ethical guidelines that apply to the journal pertain. ACS cannot be held responsible for errors or consequences arising from the use of information contained in these “Just Accepted” manuscripts.

**The influence of substituent and benzoannulation on photophysical properties of
1-benzoylmethyleneisoquinoline difluoroborates**

Borys Ośmiałowski^{a,*}, Anna Zakrzewska^a, Beata Jędrzejewska^a,
Anna Grabarz^b, Robert Zalesny^{b,c}, Wojciech Bartkowiak^b, Erkki Kolehmainen^d

^a Faculty of Chemical Technology and Engineering, UTP University of Science and
Technology, Seminaryjna 3, PL-85326 Bydgoszcz, Poland

e-mail: borys.osmialowski@utp.edu.pl or borys.osmialowski@gmail.com

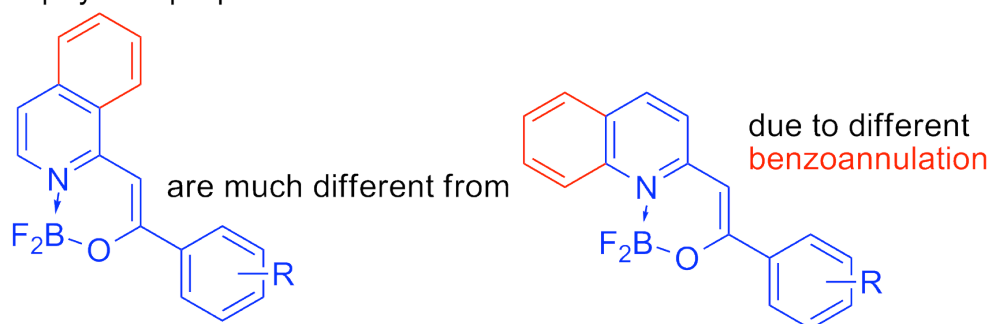
^b Faculty of Chemistry, Wrocław University of Technology, Wyb. Wyspiańskiego 27,
PL-50370 Wrocław, Poland

^c Division of Theoretical Chemistry and Biology, School of Biotechnology, Royal
Institute of Technology, SE-10691 Stockholm, Sweden

^d Department of Chemistry, P.O. Box 35, FI-40014 University of Jyväskylä, Finland

Graphical Abstract

The photophysical properties of



Abstract

A series of 1-benzoylmethyleneisoquinoline difluoroborates were synthesized and their photophysical properties were determined. The effect of the substituent and

1
2
3 benzoannulation on their properties was investigated to make a comparison with
4 recently published results focused on related quinolines. The photophysical properties
5 of isoquinoline derivatives differ from those of quinolines and most pronounced
6 differences are found for the fluorescence quantum yields. Both, experimental and
7 theoretical approaches were used to explain the observed photophysical properties.
8
9
10
11
12
13
14
15
16
17
18
19

20 Introduction

21
22 Dyes carrying BF_2 moiety are known to be fluorescent. Among them the most
23 common group are the BODIPY dyes.¹⁻³ Although plethora of studies were devoted to
24 BODIPYs, these dyes are still in a limelight. The intense studies concern not only
25 their absorption and fluorescence properties but also, for example, electrogenerated
26 chemiluminescence.⁴ On the other hand, studies for the BF_2 -carrying fluorescent dyes
27 different from BODIPYs are rare. Very recently the first survey on these molecules
28 has been published by Ziessel *et al.*⁵ Moreover, there are some attempts to clarify
29 their properties by computational approaches.⁶⁻⁸ Thus there is still a need to
30 investigate, how their properties can be tuned in order to obtain desired photophysical
31 characteristics. This is especially important for the fluorescence microscopy⁹, anion
32 sensing applications^{10,11} or bio-labeling¹², photodynamic therapy³, solar cells^{13,14} to
33 name a few. The compounds studied now contain the NBF_2O moiety.¹⁵⁻²¹ In literature
34 there exist reports on compounds where BF_2 -group is chelated also symmetrically in
35 NBF_2N ²²⁻²⁵ and OBF_2O ²⁶⁻²⁹ moieties. Also molecules carrying NBF_2O fragment,
36 especially imines based on a hydroxyl-containing Schiff bases, are known.³⁰⁻³³
37
38
39
40
41
42
43
44
45
46
47
48
49
50
51
52
53
54
55
56

57 Tailoring molecular properties by relatively simple synthetic procedures is
58 highly desirable. Systematic change of a substituent may be a successful route in
59
60

1
2
3 many instances. On the other hand, the benzoannulation may also possess a crucial
4
5 role in case of π -conjugated molecules,³⁴⁻³⁹ where it is known to have a fundamental
6
7 impact (qualitative and quantitative) on the properties of compounds exhibiting
8
9 tautomerism, for example, in heterocyclic ketones.^{37,40-43} Presumably, the properties
10
11 of BF_2 -carrying molecules may also be tuned in this way. This is due to the fact that
12
13 proton involved in the intramolecular hydrogen bonding^{40,41} can be easily replaced by
14
15 another acid such as BF_2^+ cation. The *proton-to-BF₂* exchange thus creates an
16
17 opportunity to synthesize a number of new dyes. There are several publications on
18
19 benzoannulation of the BODIPY core and its influence on photophysical properties of
20
21 these molecules.⁴⁴⁻⁴⁸ This was the inspiration to study the isomers of 2-
22
23 benzoylmethylenequinoline difluoroborates studied by us recently⁴⁹ *id est*. the 1-
24
25 benzoylmethyleneisoquinoline derivatives. It is worth mentioning that the effect of π -
26
27 electron conjugation on the fluorescence quantum yield was studied on model
28
29 compounds.⁵⁰ On the other hand, to the best of our knowledge, no detailed studies are
30
31 presented on the effect of structural isomerism on photophysical properties of BF_2 -
32
33 carrying molecules. This leads to a hypothesis that both the length and the conjugation
34
35 route should be taken into account when designing fluorescent molecules. Chart 1
36
37 depicts 1-benzoylmethyleneisoquinoline difluoroborates and their numbering. The
38
39 synthesis of the parent 1-benzoylmethyleneisoquinolines was performed as described
40
41 elsewhere for similar compounds.⁵¹ The conversion of these substrates into
42
43 fluorescent BF_2 -carrying molecules was performed as in an earlier study.^{49,52}
44
45
46
47
48
49
50
51
52
53
54
55
56
57
58
59
60

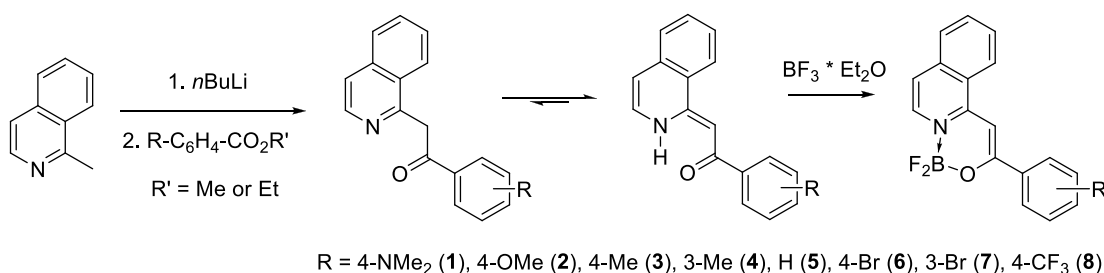


Chart 1. The reaction scheme and structures in 1-benzoylmethyleneisoquinoline difluoroborates

Results and Discussion

Linear Photophysical Properties

The photophysical properties of compounds **1–8** (Chart 1) were studied in chloroform. This solvent is known to prevent boron-ligand dissociation, exciplex formation, or photochemical reactions possible in solvents containing Lewis bases, aromatic rings, or double bonds.⁵³ Moreover, the self-aggregation is not preferred in dilute solutions as it has already been demonstrated for quinoline derivatives.⁴⁹ Figure 1 shows the absorption spectra of **1–8** and corresponding values are presented in Table 1. The molecules show absorption spectra in solution characterized by two distinct bands, the main band existing within the range 330-500 nm depending on the substituent and the second band at about 300-320 nm. Absorption spectra of complexes **2–8** exhibit fine structure although is not as distinct as in quinoline isomers, whereas **1** exhibits almost structureless band with maximum close to 460 nm. Additionally, all eight complexes have high extinction coefficients (26400-38800 M⁻¹cm⁻¹), which is typical for $\pi \rightarrow \pi^*$ transitions (Figure 1). Except **1**, the shape of the absorption spectra remains very similar to the parent compound (R=H) and it is dependent on the electron-withdrawing or electron-releasing group at different

positions in the phenyl ring. The absorption maximum and its intensity, however, differ among the studied set of compounds.

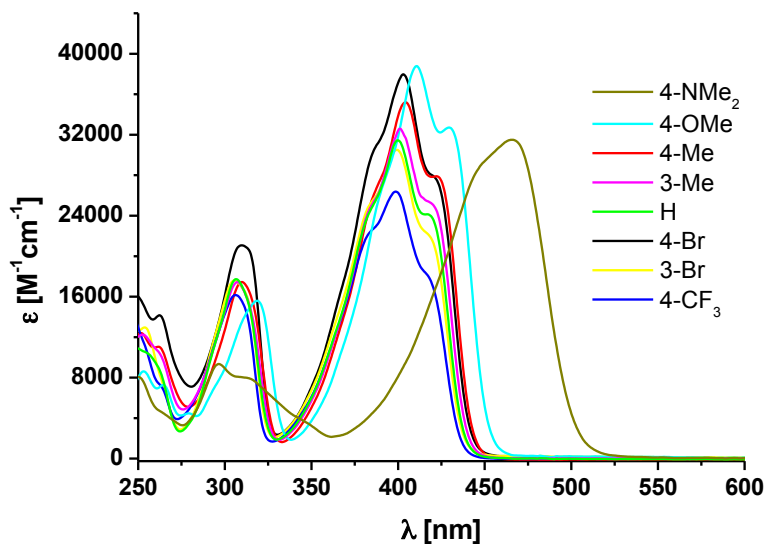


Figure 1. The electronic absorption spectra of **1-8** in CHCl_3

In order to evaluate the effect of the different substituents on the linear optical properties, $-\text{CF}_3$ was used as a benchmark acceptor group, as this moiety is the strongest acceptor in the series. In comparison with others, **8** (4-CF_3) shows similar but blue-shifted and less intense absorption band. Absorption at λ_{max} was found to progressively shift to longer wavelength upon replacing this substituent by weaker electron-withdrawing (Br) and then electron-releasing (4-Me , 4-OMe , 4-NMe_2) substituents (Table 1). This effect was accompanied by increase of the absorption intensity. A considerable red shift of the major absorption band was observed for compound **1** (4-NMe_2) (Figures 1–2). The 4-NMe_2 substituent causes a 66 nm red shift in absorption relative to the parent compound **5**. This result indicates that the absorption arises from polarized $\pi\text{-}\pi^*$ transition in the NMe_2 substituted molecule. The character of this transition will be discussed in more detail in the subsequent

section. The significant density reorganization upon excitation was prevented after the addition of gaseous HCl into the measurement cell (Figure 2) and formation of the 4-NMe₂H⁺ cation. The absorption maximum of the 4-NMe₂H⁺ derivative was blue shifted when compared with the free base and the unsubstituted congener (**5**). Similarly with another report⁴⁹, this reveals that the 4-NMe₂H⁺ group has a weak electron-acceptor properties, which is in agreement with its cationic character. This effect retracts after the addition of gaseous ammonia to a solution of protonated **1**. The similar effect was observed for 2-benzoyl(4-dimethylamino)methylenequinoline difluoroborate.⁴⁹

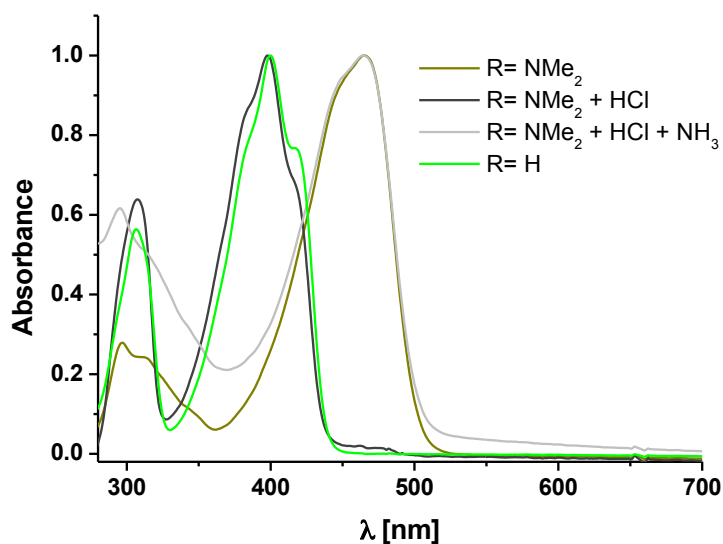
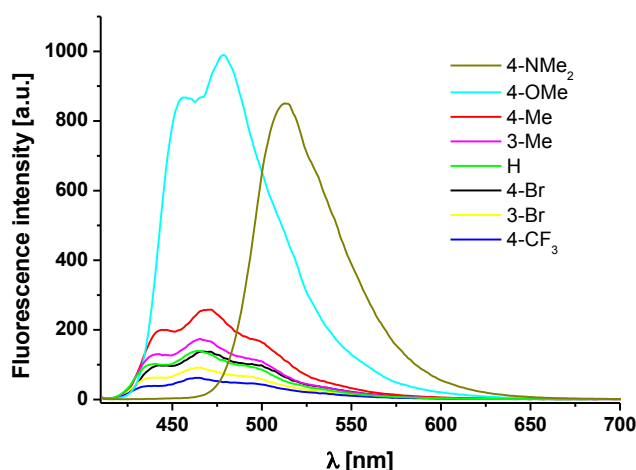


Figure 2. The comparison of the electronic absorption spectra of the parent compound (**5**), 4-NMe₂ (**1**) derivative, its HCl salt (**1**+HCl) and then neutralized with gaseous ammonia (**1**+HCl+NH₃)

Likewise, the emission spectra and fluorescence lifetimes of **1-8** were measured in chloroform. The results are given in Figure 3 and Table 1. All compounds exhibit fluorescence ranging from blue to green region. Figure 3 compares the parent compound (R=H) with its derivatives containing electron-withdrawing and electron-

1
2
3 donating groups to explore substituent effects on fluorescence spectra. As for the
4
5 absorption spectra of **1-8**, decreasing accepting strength and increasing donating
6
7 ability of the substituent results in stronger and red-shifted emission. Among them **1**
8
9 and **2** exhibit the strongest fluorescence, whereas the weakest emission occurs for
10
11 complex containing the 4-CF₃ substituent. However, the fluorescence of **1** (4-NMe₂)
12
13 is different from the others because emission spectra of **1** shows a unstructured band
14
15 (corresponding Stokes shift is 1943 cm⁻¹). The same is observed in many other
16
17 compounds including BODIPY dyes after the introduction of strong electron-donating
18
19 amino group.⁵⁴⁻⁵⁸
20
21
22
23
24
25
26



27
28
29
30
31
32
33
34
35
36
37
38
39
40
41
42
43
44
45
46
Figure 3. The fluorescence spectra of **1-8** (3-4 [μM]) in CHCl₃ λ_{ex} = 404 nm

47
48 A mirror symmetry holds between the absorption and emission spectra as
49
50 shown in Figure 4 (for compound **5**, remaining spectra are given in SI) suggesting a
51
52 weak structural relaxation of the Franck-Condon singlet excited state.
53
54
55
56
57
58
59
60

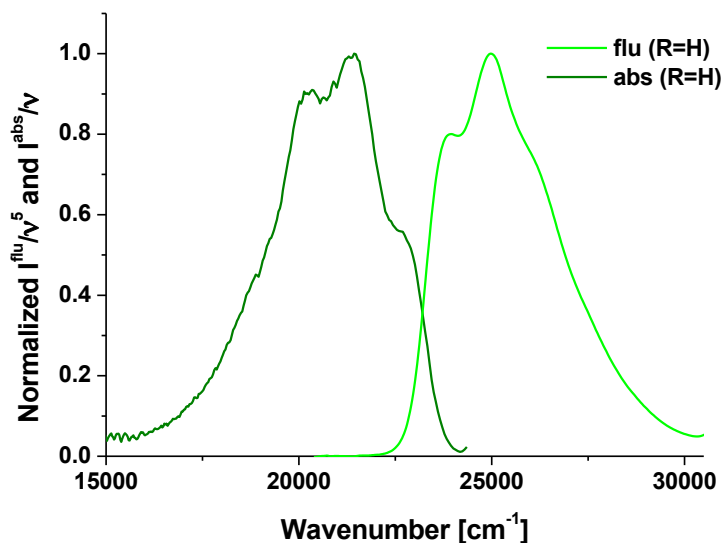


Figure 4. The normalized and scaled^{59,60} electronic absorption and fluorescence spectra of **5** in CHCl₃

Table 1. The photophysical data^a for compounds **1-8**

No	Substituent	λ_{max}^{Ab}	λ_{max}^{Fl}	$\Delta\nu^1$	$\Delta\nu^2$	ϕ_{Fl}	τ_1	τ_2	τ_{av}	χ^2	k_r	k_{nr}
		$\epsilon \cdot 10^4$					α_1	α_2				
1	4-NMe ₂	466					458	2427				
		3.15	512.4	1943 ^b	0.743	4.33	95.67	2341.7	1.83	3.17	1.10	
2	4-OMe	410.5					405	1061				
		3.88	478.2	1320	3449	0.313	15.75	84.25	957.7	1.29	3.26	7.18
3	4-Me	404					348	747				
		3.52	471	1113	3521	0.087	92.82	7.18	376.7	1.28	2.32	24.23
4	3-Me	401.5					242	825				
		3.26	464.8	1077	3392	0.060	98.27	1.73	252.1	1.17	2.37	37.30
5	H	400					191	1109				
		3.14	463.2	1139	3411	0.046	98.77	1.23	202.3	1.16	2.28	47.15
6	4-Br	403					211	1374				
		3.80	466.4	1118	3373	0.049	98.19	1.81	232.1	1.12	2.10	41.00
7	3-Br	399.5					154	1249				
		3.05	465	1082	3526	0.033	97.33	2.67	183.2	1.50	1.82	52.76
8	4-CF ₃	398.5					127	1053				
		2.64	464.6	1092	3570	0.026	98.63	1.37	139.7	1.20	1.88	69.71

^a - Absorption ($\lambda_{max}^{Ab}; nm$), Fluorescence Maxima ($\lambda_{max}^{Fl}; nm$), shift ($\Delta\nu, cm^{-1}$), Maximum Extinction Coefficient ($\epsilon; M^{-1}cm^{-1}$), Fluorescence Quantum Yield (ϕ_{Fl}), Fluorescence Lifetime ($\tau; ps$), their amplitudes (α) and correlation coefficients (χ^2), Radiative ($k_r; 10^8 s^{-1}$) and Non-radiative ($k_n; 10^8 s^{-1}$) Rate Constants. ^b difference between positions of the band maxima of the absorption and emission spectra of 4-NMe₂.

The fluorescence quantum yield was determined relative to coumarine 1 quantum counter ($\phi_{ref} = 0.64$) with excitation at 404 nm. Derivatives **1** and **2** exhibit good fluorescence quantum yield (0.74 and 0.31) whereas for the others it is lower by one order of magnitude.

Figure 5 shows the biexponential fluorescence decay curve for **5**. The same is used for the fitting of other derivatives. An additional long-lived component that appeared in these compounds suggests a complex photophysical processes. The fluorescence lifetimes measured by time correlated single photon counting method are shown in Table 1 above.

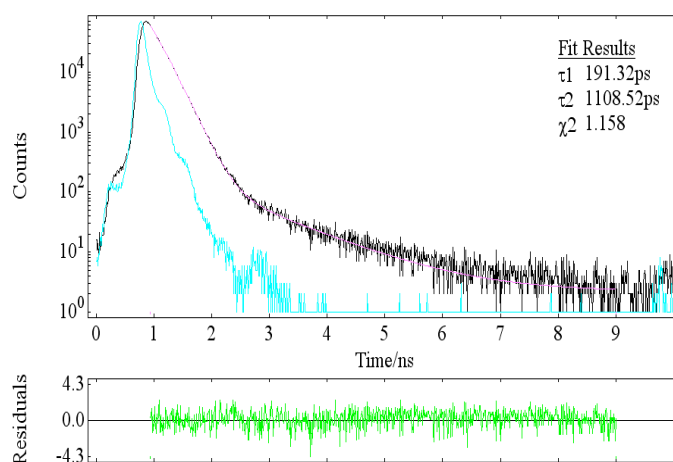


Figure 5. The fluorescence decay curve for **5** recorded in CHCl₃; $\lambda_{ex} = 404$ nm; $\lambda_{em} = 450$ nm

In the parent compound (**5**), ϕ_{Fl} and τ_{Fl} are 0.046 and 191 ps (major component), respectively. These values are diminished to 0.026 and 127 ps, respectively, when the 4-CF₃ group is present (**8**). Hence, the rate constant of radiative k_r deactivation is decreased from 2.28×10^8 to $1.82 \times 10^8 s^{-1}$, respectively caused by strongly electron-

1
2
3 withdrawing character of the substituent. On the other hand, introducing an electron-
4 releasing substituent enhances the fluorescence quantum yields, lifetimes and Stokes'
5 shift, *e.g.* for 4-NMe₂ the $\phi_{\text{Fl}}=0.74$, $\tau_{\text{Fl}}=2427$ ps (major component of different nature
6 than that in **3-8**, see Table 1 for τ_1 and τ_2) and $\Delta\nu=1943$ cm⁻¹. In both ϕ_{Fl} and τ_{Fl} show
7 the monotonous increase with the increase in electron-donating abilities of the
8 substituent. Additionally, the data compiled in Table 1 show that for tested
9 compounds the non-radiative transition rates are of the same order as the radiative
10 ones only for **1** and **2**. In case of others, the non-radiative transition rates are at least
11 one order of magnitude larger than the radiative ones, which indicates contribution of
12 the excited singlet state that deactivate by the internal conversion processes.
13
14
15
16
17
18
19
20
21
22
23
24
25
26

27 The complexes studied here can be grouped into two categories. One includes
28 compound **1** that is characterized by rather large Stokes shifts with long radiative
29 lifetimes and the low-energy emissions, and **2-8** that have the high-energy emissions
30 and short fluorescence lifetimes. This suggests that emissions arise from different
31 types of excited states. Presumably, an increase in π conjugation length typically
32 results in a red shift of emission and change in corresponding quantum yield.⁵⁰ The
33 spectra roughly follow this rule but some exceptions were also observed. For
34 example, the donating substituent carrying a lone-electron pair as in **1** extends the
35 electron conjugation with respect to that in **5**. Moreover, this allows efficient
36 polarization of the electronic density upon excitation leading to the largest red-shifted
37 emission. However, the length of conjugation is not the only parameter that influences
38 the emissive state energy of the complexes. The inductive effects or mentioned charge
39 transfer should be also taken into account.
40
41
42
43
44
45
46
47
48
49
50
51
52
53
54
55
56

57 As stated above, distinct red features in the absorption spectrum for **1** is ascribed to
58 substantial density change in the π - π^* excited state. These features are dominated by
59
60

1
2
3 excitations in which charge is transferred from donor (4-NMe₂) to the acceptor
4 (NBF₂O) moiety. These observations further support the same interpretation for 4-
5
6 OMe derivative (**2**) where reorganization of electron density is less efficient than that
7
8 in **1**. From the fluorescence spectra, the emission maximum of **1** is red-shifted by 34
9
10 nm compared to that for **2**. Although the electron donating 4-OMe does not seem to
11
12 make such a significant effect as 4-NMe₂, the radiative lifetimes follow the expected
13
14 trend showing some differences in the quantum yield and fluorescence decay. For **1**,
15
16 τ_2 is more than twice the value for **2**, indicating a large long-lived contribution coming
17
18 from the effect of strong electron donating group. The more electron-rich **1** (versus **5**)
19
20 may slightly weaken the acceptor ability of the NBF₂O moiety, thus increasing the
21
22 energy of the transition. Within all **1-8**, where $\pi \rightarrow \pi^*$ transitions dominate the
23
24 electronic transitions, the 4-OMe exerts a subtle but measurable effect on fluorescence
25
26 decay whereas the 4-NMe₂ has significant effect on the excited state properties.
27
28
29
30
31
32
33

34 The obtained results suggest that there may be two excited-state conformers for
35
36 these compounds. One has a structure conducive to the $\pi \rightarrow \pi^*$ state being lowest
37
38 energy in the excited state and gives rise to a short-lived (127-458 ps) $\pi \rightarrow \pi^*$
39
40 fluorescence. The structure dominates for 1-benzoylmethyleneisoquinoline
41
42 difluoroborates bearing electron-withdrawing substituents and weak electron-
43
44 releasing group. Its share of average fluorescence lifetime is in the range 99-93%. In
45
46 the case of compounds containing strong electron-donor (4-NMe₂) the dominant
47
48 structure gives an transition associated with substantial charge reorganization and is
49
50 the source of the much longer-lived emission (2.5 ns). While one could expect the
51
52 systematic changes of properties related to the substituent alteration, here some kind
53
54 of the sudden drop of properties is observed when passing from 4-Me via 4-OMe to 4-
55
56 NMe₂. This suggests the existence of two very different in character fluorescence
57
58
59
60

1
2
3 individuals in the latter derivative. A possible scenario is that a conformer with
4 twisted NMe₂ group (or C₆H₄NMe₂) exists.⁶¹⁻⁶³ The excited-state geometry
5 optimization of 4-NMe₂ (at the CAM-B3LYP/6-311++G(d,p) level of theory)
6 revealed an existence of stable conformer with NMe₂ group co-planar with phenyl
7 ring. Calculated Stokes shift (48 nm) was found to be in excellent agreement with
8 experimental value (46 nm).
9
10
11
12
13
14
15
16

17 In summary, the intensity of the absorption and emission bands increases with
18 increasing electron-donating properties of the substituent in phenyl moiety, and the
19 maxima of the bands are red shifted. A greater disparity in electron-donating ability of
20 the 4-NMe₂ group seems to result in a stronger transition with charge reorganization
21 dominated by the more electron-rich aryl group. However, the $\pi \rightarrow \pi^*$ transitions
22 dominate for other 1-benzoylmethyleneisoquinoline difluoroborates.
23
24
25
26
27
28
29
30
31
32
33

34 *Comparisons of isoquinolines with quinolines*

35 For the comparison purposes and in order to gain a further insight into the
36 properties of **1-8** a series of charts were drawn (SI). The properties of 2-
37 benzoylmethylenequinoline difluoroborates were used for that purposes.⁴⁹ These
38 comparisons allow to draw the following conclusions for *the NMR-derived data*: a)
39 the ¹⁵N chemical shift (sensitive to environment⁶⁴) is linearly dependent (correlation
40 coefficient R=0.99, **5** and **8** excluded) on the substituent constant with similar slope
41 between the series but different intercept (Chart S1), b) the same applies for other
42 chemical shifts as, for example, ¹⁹F data (R=0.90, **1** excluded from correlation), ¹³C of
43 carbon no. 1 in isoquinoline (R=0.98), CO (R=0.95) and methine CH carbon
44 (R=0.95) atoms, while *for the photophysical data* it can be concluded: a) the
45 fluorescence quantum yields are, in general, higher for quinoline derivatives than that
46
47
48
49
50
51
52
53
54
55
56
57
58
59
60

1
2
3 for isoquinolines (Chart S2), *b*) the data of the radiative and non-radiative rate
4 constants suggest the non-radiative mechanism dominates (Chart S3) and is
5 responsible for much lower fluorescence quantum yield (Chart S4) in isoquinolines, *c*)
6 for the fluorescence lifetimes opposite effect is observed between short and long lived
7 species, *id est* the correlation with the substituent constant is observed for short
8 lifetime in isoquinolines ($R=0.93$) and for the long lifetime for quinolines ($R=0.97$,
9 Chart S6). The above-mentioned observations lead to the conclusion that variable
10 benzoannulation causes dramatic changes in the photophysical properties of studied
11 molecules. One mechanism that can cause a sudden drop in the fluorescence quantum
12 yield is high non-radiative processes caused by vibrations of the molecular skeleton or
13 by much stronger interaction of the BF_2 moiety with the solvent molecules (compare
14 the topology of these derivatives). The detailed studies on these effects are under
15 progress.

36 *Quantum-chemical calculations*

37
38
39
40
41 In order to support experimental data, the quantum chemical calculations were
42 performed. In particular, one of the primary aims behind these computations was to
43 analyze the vibrational fine structure of absorption band related to lowest-lying $\pi \rightarrow \pi^*$
44 transition and the associated changes in electronic density. The oscillator strength (f)
45 accompanying this transition is rather large for all studied molecules and is presented
46 in Table 2. It should be highlighted that the largest probability was observed for the
47 one-electron HOMO \rightarrow LUMO excitation. The frontier orbitals involved in $\pi \rightarrow \pi^*$
48 transition for **1** and **5** are shown in Table 3 (a complete dataset for all molecules is
49 presented in SI). As seen in accordance with previous conclusions based on
50
51
52
53
54
55
56
57
58
59
60

1
2
3 experimental data, much more significant density change upon excitation is found for
4 4-NMe₂ substituent. In order to put these changes on a quantitative basis, the fragment
5 analysis of frontier molecular orbitals involved in the excitation was performed (cf.
6 section *Computational details*). It follows from this analysis that the net charge
7 transferred from fragment **B** to fragment **A** (Fig. 6) upon excitation is 0.47e and
8 0.045e for compound **1** and **5**, respectively.
9
10
11
12
13
14
15
16
17
18
19

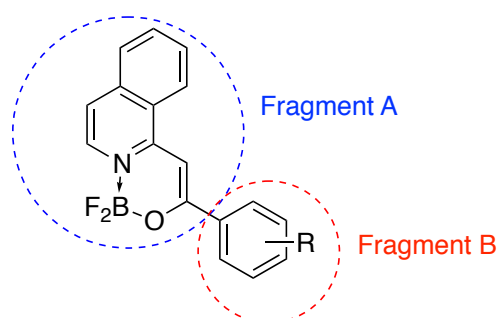


Figure 6. Scheme of the decomposition of molecule into fragments

Although the comparison of computed vertical excitation energy with experimental absorption band maxima still remains the most common route, critical assessment of this approach has already been performed by some authors.⁶⁵⁻⁶⁷ In Table 2 there is presented the wavelength corresponding to vertical excitation (computed without zero-point vibrational energy included) and wavelength related to the adiabatic transition (within the IMDHO model the latter value corresponds to the 0-0 excitation). The results clearly show that the B3LYP functional provides the most accurate estimation of experimental absorption/fluorescence crossing point (referred to as 0-0 energy). The other two functionals significantly overestimate the 0-0 energy; the largest deviation from experimental data is found for compound **1**, characterized by significant charge reorganization upon excitation. Other groups have reported the accurate estimation of the spectroscopic parameters (within TD-DFT scheme) for the cyanine-like molecules (such as BODIPY).⁶⁸⁻⁷³

Table 2. Calculated spectroscopic parameters corresponding to the lowest lying ($\pi \rightarrow \pi^*$) excited state where λ_v and λ_{ad} correspond to vertical and adiabatic transition.

Substituent (comp.)	Functionals									exp. λ_{0-0} [nm]
	B3LYP			CAM-B3LYP			PBE0			
	λ_v [nm]	λ_{ad} [nm]	f	λ_v [nm]	λ_{ad} [nm]	f	λ_v [nm]	λ_{ad} [nm]	f	
4-NMe ₂ (1)	460	477	0.985	394	430	1.118	422	438	1.042	491
4-OMe (2)	412	437	0.896	367	411	0.955	398	424	0.920	442
4-Me (3)	401	440	0.812	360	395	0.858	388	423	0.830	438
3-Me (4)	396	426	0.744	360	397	0.817	385	415	0.764	431
H (5)	395	426	0.726	356	390	0.781	383	413	0.745	429
4-Br (6)	400	438	0.856	359	397	0.889	388	423	0.875	432
3-Br (7)	395	438	0.743	356	393	0.798	386	414	0.780	430
4-CF ₃ (8)	397	432	0.739	355	393	0.789	384	418	0.745	427

In order to gain an insight into the structure of experimentally recorded absorption bands, we have also performed simulation of their vibrational fine structure. The results are presented in Fig. 7 and 8. In the case of all performed simulations, the homogenous broadening was set to 100 cm⁻¹ and standard deviation of the distribution of 0-0 excitation energies corresponding to inhomogeneous broadening was chosen as 420 (**6**), 450 (**2, 3, 5, 7, 8**) 475 (**4**) or 500 cm⁻¹ (**1**) to correctly reproduce the overall absorption band shapes. As can be seen in Fig. 7, among three employed functionals, only CAM-B3LYP satisfactorily predicts the vibrational fine structure of absorption band corresponding to the $\pi \rightarrow \pi^*$ transition. Two other functionals incorrectly determine the intensity ratio for major band shoulders. Within the framework of applied model it can be directly related to the displacements between the potential energy surfaces, which are computed based on the excited-state gradients. The differences between the experimental band shape and the profiles simulated using B3LYP and PBE0 functionals may indicate, indirectly, that the latter two functionals have difficulties in predicting excited-state gradients. Thus, CAM-B3LYP functional

was used to simulate the band shapes for all series of compounds (cf. Fig. 8), which are in good accordance with experimental spectra presented in Fig. 1.

Table 3. Kohn-Sham frontier orbitals determined using B3LYP functional and 6-311++G(d,p) basis set at the contour surfaces of orbital amplitude 0.04 e/bohr³

Compound	HOMO	LUMO
1 (4-NMe ₂)		
5 (H)		

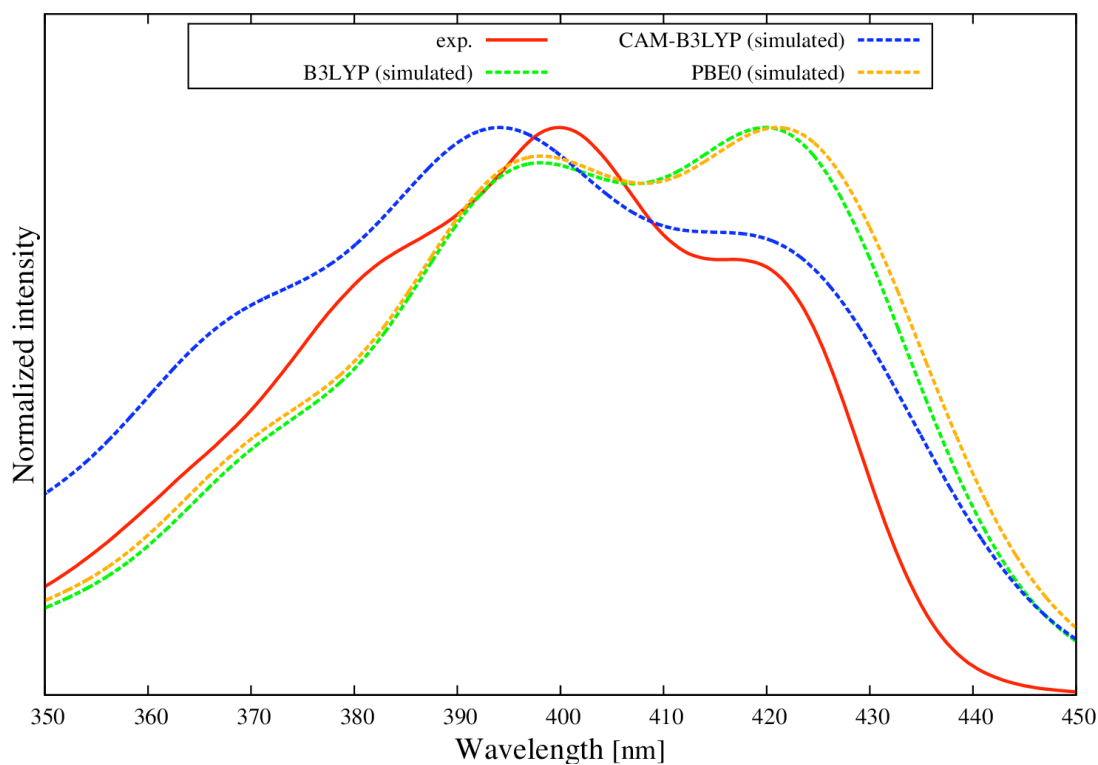


Figure 7. Comparison of experimental and simulated absorption spectra for R=H derivative. The spectra were shifted to match the experimental long-wavelength feature

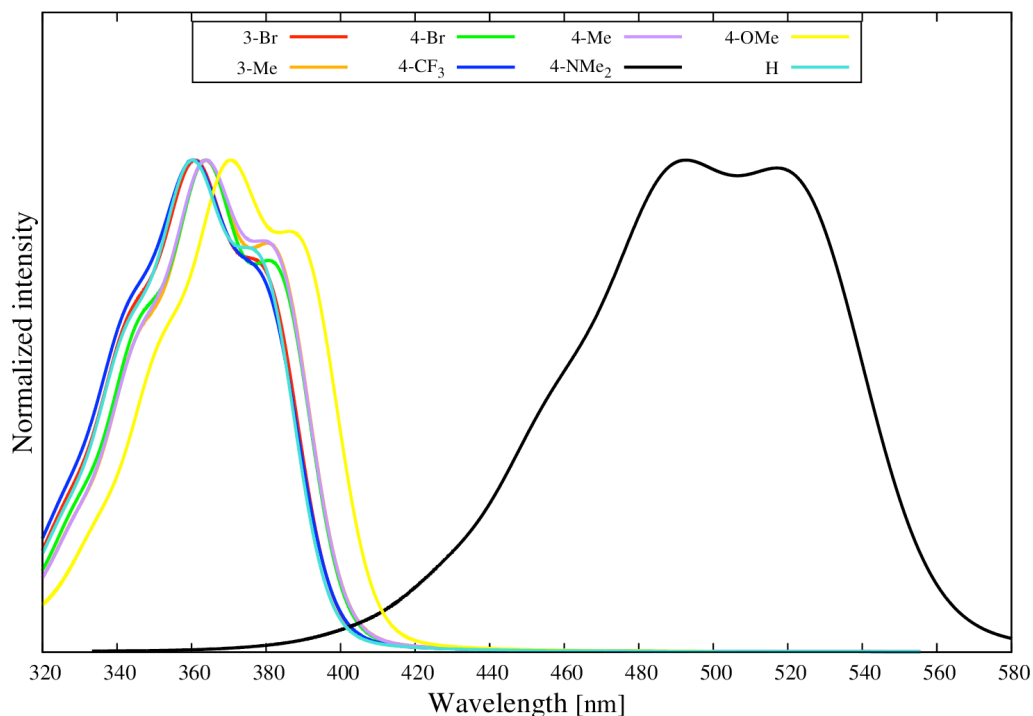


Figure 8. Absorption spectra simulated using CAM-B3LYP functional

Conclusions

The spectral and computational data show that the absorption and fluorescence properties of substituted 1-benzoylmethyleneisoquinoline difluoroborates are similar to those in quinoline derivatives while some small spectral shifts are noticed. The most dramatic differences between quinoline and isoquinoline derivatives are within their fluorescence quantum yield, which decreases quickly when going from strong to weak electron donating substituent. This shows that isoquinolines are less attractive for their use as fluorescent probes. Moreover, this also shows that a special care should be paid not only to the substituent applied, degree of π -electron conjugation, benzoannulation but also to the way the benzoannulation takes place. This clearly influences the synthetic procedures that would lead to materials with desired properties. The correlations of the NMR chemical shifts with substituent constants are similar as in quinolines making the substituent effect in the ground state similar

1
2
3 between these series It has been found that only CAM-B3LYP functionals yields the
4 correct absorption band shape for studied molecules.
5
6

7 8 **Experimental** 9

10 The 1-benzoylmethyleneisoquinoline difluoroborates were synthesized as
11 before (ketone synthesis⁵¹; complexation²²). The same applies for visible⁴⁹ and
12 NMR⁵² spectral measurements. Electronic structure calculations were performed
13 using the Kohn-Sham formulation of density functional theory. In order to take into
14 account the conditions of experimental measurements, the calculation were carried
15 out in the presence of the solvent, using the linear response polarizable continuum
16 model (LR-PCM⁷⁴). Comparison of linear LR-PCM with more accurate corrected LR-
17 PCM can be found in recent paper by Chibani et al..⁷⁵ Optimization of the ground
18 state geometry was carried out using three different exchange-correlation functionals:
19 B3LYP, CAM-B3LYP, and PBE0. Vertical excitation energies were computed
20 employing the time-dependent density functional theory. For all quantum-chemical
21 calculations 6-311++G(d,p) basis set was used. All electronic structure calculations
22 were performed using Gaussian 2009 D01 program.⁷⁶ Additionally, in order to
23 simulate the vibrational structure of the absorption spectra, *orca_asa* program was
24 used (the part of ORCA package).⁷⁷ Simulations of the absorption bands, interrelated
25 with transitions to the (π - π^*) excited state, were performed using Independent Mode
26 Displaced Harmonic Oscillator (IMDHO) approximation. In the case of ground
27 electronic state, the entire set of normal modes of vibration was included in
28 simulations. Dimensionless normal coordinate displacements ($\Delta_{Q,k}$) for excited-state
29 with respect to the ground state equilibrium geometry were calculated using custom
30 software as follows:
31
32
33
34
35
36
37
38
39
40
41
42
43
44
45
46
47
48
49
50
51
52
53
54
55
56
57
58
59
60

$$\Delta_{Q,k} = -\frac{1}{\omega_{ek}^2} \left[\frac{\partial E}{\partial Q_k} \right]_{Q=0}$$

where $\left[\frac{\partial E}{\partial Q_k} \right]_{Q=0}$ corresponds to excited-state potential energy gradient along the k -th normal mode at the ground-state geometry. The energy of adiabatic transition was computed according to the following formula:

$$\Delta E_{ad} = \Delta E_v - \sum_k \frac{\omega_k}{2} \Delta_k^2$$

In this study we also present a fragment analysis of the molecular orbitals. It is carried out under the assumption that one can divide molecular structure into N fragments. The electronic density may then be decomposed and described by means of atomic orbitals centred on nuclei corresponding to the fragments. Fragment contribution is computed as⁷⁸:

$$C_{frag} = \sum_j^{n_{frag}} c_j^2 + \sum_j^{n_{frag}} \sum_{i < j}^{n_{frag}} 2c_i c_j S_{ij}$$

where i and j run over the n_{frag} basis set atomic orbitals, c_i is the coefficient by which the basis function enters the molecular orbital and S_{ij} is the basis set overlap matrix element.

Compounds Characterization

All compounds were obtained²² as described for quinoline derivatives.⁴⁹ The reaction yields (after purification) varied between 35 and 45%. The typical procedure was as follows: to the magnetically stirred solution (nitrogen atmosphere) of substituted 1-benzoylmethyleneisoquinoline (1g) in dry chloroform (15-20 ml) and N-ethyl-diisopropylamine (two equivalents) BF_3 etherate (two equivalents) was added.

The solution was stirred overnight at room temperature and then concentrated Na_2CO_3

1
2
3 water solution (20ml) was added slowly to the mixture. The organic fraction was
4
5 separated, water layer extracted with chloroform (two times using ca. 20-30 ml),
6
7 dried (Na₂SO₄) and evaporated under reduced pressure. Residual solids were purified
8
9 by flash chromatography (SiO₂) using acetonitrile (**1**) or DCM (**2-8**) as an eluent.
10
11

12 *1-(4-Dimethylamino)benzoylmethyleneisoquinoline difluoroborate (1)* 0.52g
13 (44.6%). ¹H NMR (DMSO-*d*₆ from TMS) δ: 8.92 (d, 1H, ³J_{H,H}=8.3Hz), 8.07 (d, 2H,
14 ³J_{H,H}=9.0Hz), 8.02-7.97 (m, 2H), 7.83 (t, 1H), 7.68 (d, 1H, ³J_{H,H}=6.8Hz), 7.46 (s, 1H),
15 6.82 (d, 2H, ³J_{H,H}=9.0Hz), 3.06 (s, 6H). ¹¹B NMR (DMSO-*d*₆ from BF₃·Et₂O) δ:
16 1.588 (t), ¹³C NMR (DMSO-*d*₆ from TMS) δ:165.8, 152.9, 152.8, 136.5, 134.3, 131.4,
17 129.5, 129.2,127.8, 127.3, 123.8, 120.7, 117.8, 111.9, 87.4, ca. 40 (overlapped with
18 solvent signal), ¹⁵N (DMSO-*d*₆ from MeNO₂) δ: -196.3, ¹⁹F NMR (DMSO-*d*₆ from
19 CFCl₃) δ: -138.3. Mp 260.1-263.8°C. Anal. Calcd for C₁₉H₁₇BF₂N₂O: C, 67.48; H,
20 5.07; N, 8.28. Found: C, 67.41; H, 5.11; N, 8.20.
21
22
23
24
25
26
27
28
29
30
31
32
33
34

35 *1-(4-Methoxy)benzoylmethyleneisoquinoline difluoroborate (2)* 0.41g (35.0%).
36 ¹H NMR (CDCl₃ from TMS) δ: 8.40 (d, 1H, ³J_{H,H}=8.3Hz), 8.17 (d, 1H, ³J_{H,H}=5.4Hz),
37 8.04 (d, 2H, ³J_{H,H}=8.9Hz), 7.87 (t, 1H), 7.84 (t, 1H), 7.74 (t, 1H), 7.47 (d, 1H,
38 ³J_{H,H}=6.8Hz), 7.08 (s, 1H), 6.98 (d, 2H, ³J_{H,H}=8.9Hz), 3.89 (s, 3H). ¹¹B NMR (CDCl₃
39 from BF₃·Et₂O) δ: 1.762 (t), ¹³C NMR δ: 165.9, 162.5, 152.7, 136.6, 133.4, 131.6,
40 128.9, 128.7, 127.5, 126.8, 125.6, 123.8, 117.8, 114.0, 88.0, 55.5. ¹⁵N NMR (CDCl₃
41 from MeNO₂) δ: -193.6, ¹⁹F NMR (CDCl₃ from CFCl₃) δ: -139.05. Mp 236.5-
42 238.7°C. Anal. Calcd for C₁₈H₁₄BF₂NO₂: C, 66.50; H, 4.34; N, 4.31. Found: C, 66.39;
43 H, 4.52; N, 4.23.
44
45
46
47
48
49
50
51
52
53
54
55
56

57 *1-(4-Methyl)benzoylmethyleneisoquinoline difluoroborate (3)* 0.49g (41.4%).
58 ¹H NMR (CDCl₃ from TMS) δ: 8.42 (d, 1H, ³J_{H,H}=8.4Hz), 8.21 (d, 1H, ³J_{H,H}=5.6Hz),
59 7.98 (d, 2H, ³J_{H,H}=8.4Hz), 7.89 (t, 1H), 7.86 (t, 1H), 7.76 (t, 1H), 7.51 (d, 1H,
60

³J_{H,H}=6.8Hz), 7.30 (d, 2H, ³J_{H,H}=8.4Hz), 7.15 (s, 1H), 2.45 (s, 3H). ¹¹B NMR (CDCl₃ from BF₃·Et₂O) δ: 1.787 (t), ¹³C NMR δ: 166.1, 152.7, 142.1, 136.5, 133.4, 131.6, 131.5, 129.3, 128.8, 127.5, 127.0, 125.7, 123.8, 118.1, 88.8, 21.5. ¹⁵N NMR (CDCl₃ from MeNO₂) δ: -192.5. ¹⁹F NMR (CDCl₃ from CFCl₃) δ: -138.7. Mp 231.2-233.5°C. Anal. Calcd for C₁₈H₁₄BF₂NO: C, 69.94; H, 4.56; N, 4.53. Found: C, 69.75; H, 4.71; N, 4.44.

1-(3-Methyl)benzoylmethyleneisoquinoline difluoroborate (4) 0.51g (43.1%).

¹H NMR (CDCl₃ from TMS) δ: 8.43 (d, 1H, ³J_{H,H}=8.7Hz), 8.21 (d, 1H, ³J_{H,H}=6.8Hz), 7.90-7.84 (overlapped signals, 4H), 7.76 (t, 1H), 7.52 (d, 1H, ³J_{H,H}=6.8Hz), 7.37 (t, 1H), 7.31 (d, 1H, ³J_{H,H}=7.6Hz), 7.16 (s, 1H), 2.45 (s, 3H). ¹¹B NMR (CDCl₃ from BF₃·Et₂O) δ: 1.800 (t), ¹³C NMR δ: 166.1, 152.6, 138.4, 136.6, 134.3, 133.5, 132.3, 131.7, 128.9, 128.5, 127.6, 127.5, 125.7, 124.1, 123.8, 118.4, 89.3, 21.4. ¹⁵N NMR (CDCl₃ from MeNO₂) δ: -192.2. ¹⁹F NMR (CDCl₃ from CFCl₃) δ: -138.6. Mp 215.6-218.4°C. Anal. Calcd for C₁₈H₁₄BF₂NO: C, 69.94; H, 4.56; N, 4.53. Found: C, 69.81; H, 4.78; N, 4.49.

1-Benzoylmethyleneisoquinoline difluoroborate (5) 0.49g (41.1%). ¹H NMR

(CDCl₃ from TMS) δ: 8.42 (d, 1H, ³J_{H,H}=8.5Hz), 8.22 (d, 1H, ³J_{H,H}=6.1Hz), 8.07 (d, 2H, ³J_{H,H}=8.2Hz), 7.89 (t, 1H), 7.86 (t, 1H), 7.76 (t, 1H), 7.53 (d, 1H, ³J_{H,H}=6.8Hz), 7.51-7.45 (m, 3H), 7.17 (s, 1H). ¹¹B NMR (CDCl₃ from BF₃·Et₂O) δ: 1.805 (t), ¹³C NMR δ: 165.9, 152.6, 136.6, 134.4, 133.5, 131.7, 131.5, 128.9, 128.6, 127.5, 126.9, 125.7, 123.8, 118.5, 89.3. ¹⁵N NMR (CDCl₃ from MeNO₂) δ: -195.7. ¹⁹F NMR (CDCl₃ from CFCl₃) δ: -138.6. Mp 233.7-236.8°C. Anal. Calcd for C₁₇H₁₂BF₂NO: C, 69.19; H, 4.10; N, 4.75. Found: C, 69.13; H, 4.06; N, 4.70.

1-(4-Bromo)benzoylmethyleneisoquinoline difluoroborate (6) 0.50g (43.6%).

¹H NMR (CDCl₃ from TMS) δ: 8.42 (d, 1H, ³J_{H,H}=8.4Hz), 8.24 (d, 1H, ³J_{H,H}=6.8Hz),

1
2
3 7.94-7.87 (m, 4H), 7.80 (t, 1H), 7.60 (d, 2H, $^3J_{H,H}=8.5\text{Hz}$), 7.58 (d, 1H, $^3J_{H,H}=6.6\text{Hz}$),
4
5 7.16 (s, 1H). ^{11}B NMR (CDCl_3 from $\text{BF}_3\cdot\text{Et}_2\text{O}$) δ : 1.750 (t), ^{13}C NMR δ : 164.5, 152.3,
6
7 136.7, 133.7, 133.3, 131.9, 131.7, 129.1, 128.4, 127.6, 126.1, 125.6, 123.8, 118.8,
8
9 89.5. ^{15}N NMR (CDCl_3 from MeNO_2) δ : -190.4. ^{19}F NMR (CDCl_3 from CFCl_3) δ : -
10
11 138.5. Mp 231.8-234.9°C. Anal. Calcd for $\text{C}_{17}\text{H}_{11}\text{BBrF}_2\text{NO}$: C, 54.60; H, 2.96; N,
12
13 3.75. Found: C, 54.53; H, 3.01; N, 3.67.

14
15
16
17
18 *1-(3-Bromo)benzoylmethyleneisoquinoline difluoroborate (7)* 0.44g (38.4%).

19
20 ^1H NMR (CDCl_3 from TMS) δ : 8.44 (d, 1H, $^3J_{H,H}=8.3\text{Hz}$), 8.25 (d, 1H, $^3J_{H,H}=6.3\text{Hz}$),
21
22 8.20 (m, 1H), 7.99 (d, 1H, $^3J_{H,H}=8.0\text{Hz}$), 7.94-7.86 (m, 2H), 7.80 (t, 1H), 7.63 (d, 1H,
23
24 $^3J_{H,H}=8.0\text{Hz}$), 7.59 (d, 1H, $^3J_{H,H}=6.8\text{Hz}$), 7.36 (t, 1H), 7.15 (s, 1H). ^{11}B NMR (CDCl_3
25
26 from $\text{BF}_3\cdot\text{Et}_2\text{O}$) δ : 1.748 (t), ^{13}C NMR δ : 164.0, 152.3, 136.7, 136.4, 134.2, 133.7,
27
28 131.8, 130.1, 129.8, 129.1, 127.6, 125.7, 125.5, 123.8, 122.9, 119.1, 90.0. ^{15}N NMR
29
30 (CDCl_3 from MeNO_2) δ : -189.8. ^{19}F NMR (CDCl_3 from CFCl_3) δ : -138.5. Mp 227.5-
31
32 229.2°C. Anal. Calcd for $\text{C}_{17}\text{H}_{11}\text{BBrF}_2\text{NO}$: C, 54.60; H, 2.96; N, 3.75. Found: C,
33
34 54.48; H, 3.09; N, 3.68.

35
36
37
38
39 *1-(4-Trifluoromethyl)benzoylmethyleneisoquinoline difluoroborate (8)* 0.48g

40
41 (41.7%). ^1H NMR (CDCl_3 from TMS) δ : 8.44 (d, 1H, $^3J_{H,H}=8.5\text{Hz}$), 8.26 (d, 1H,
42
43 $^3J_{H,H}=6.6\text{Hz}$), 8.12 (d, 2H, $^3J_{H,H}=8.3\text{Hz}$), 7.93 (t, 1H), 7.88 (d, 1H, $^3J_{H,H}=7.5\text{Hz}$), 7.81
44
45 (t, 1H), 7.69 (d, 2H, $^3J_{H,H}=8.3\text{Hz}$), 7.59 (d, 1H, $^3J_{H,H}=6.6\text{Hz}$), 7.22 (s, 1H). ^{11}B NMR
46
47 (CDCl_3 from $\text{BF}_3\cdot\text{Et}_2\text{O}$) δ : 1.770 (t), ^{13}C NMR δ : 163.6, 152.1, 137.6, 136.7, 133.8,
48
49 132.7, 131.7, 129.2, 127.6, 127.0, 125.7, 125.5, 125.14, 123.8, 122.4, 119.4, 90.6. ^{15}N
50
51 NMR (CDCl_3 from MeNO_2) δ : -190.5. ^{19}F NMR (CDCl_3 from CFCl_3) δ : -138.2, -
52
53 62.9. Mp 230.9-234.2°C. Anal. Calcd for $\text{C}_{18}\text{H}_{11}\text{BF}_5\text{NO}$: C, 59.54; H, 3.05; N, 3.86.
54
55 Found: C, 59.45; H, 3.14; N, 3.81.
56
57
58
59
60

Supporting Information

NMR spectra, correlation and comparison charts, fluorescence decay spectra, computational results and Cartesian coordinates. This material is available free of charge via the Internet at <http://pubs.acs.org>.

Acknowledgments

Financial support from the National Science Centre (Grant No. 2013/09/B/ST5/03550) is gratefully acknowledged. This research was supported by PL-Grid Infrastructure and the Wroclaw Center for Networking and Supercomputing. R.Z. is a Wenner-Gren Foundations scholar.

References

- (1) Loudet, A.; Burgess, K. *Chem. Rev.* **2007**, *107*, 4891.
- (2) Boens, N.; Leen, V.; Dehaen, W. *Chem. Soc. Rev.* **2012**, *41*, 1130.
- (3) Kamkaew, A.; Lim, S. H.; Lee, H. B.; Kiew, L. V.; Chung, L. Y.; Burgess, K. *Chem. Soc. Rev.* **2013**, *42*, 77.
- (4) Nepomnyashchii, A. B.; Bard, A. J. *Acc. Chem. Res.* **2012**, *45*, 1844.
- (5) Frath, D.; Massue, J.; Ulrich, G.; Ziessel, R. *Angew. Chem. Int. Ed.* **2014**, *53*, 2290.
- (6) Jacquemin, D.; Chibani, S.; Le Guennic, B.; Mennucci, B. *J. Phys. Chem. A* **2014**, *118*, 5343.
- (7) Chibani, S.; Laurent, A. D.; Le Guennic, B.; Jacquemin, D. *J. Chem. Theory Comput.* **2014**, *10*, 4574.
- (8) Laurent, A. D.; Adamo, C.; Jacquemin, D. *Phys. Chem. Chem. Phys.* **2014**, *16*, 14334.
- (9) Nie, S.; Chiu, D. T.; Zare, R. N. *Anal. Chem.* **1995**, *67*, 2849.
- (10) Ozdemir, T.; Sozmen, F.; Mamur, S.; Tekinay, T.; Akkaya, E. U. *Chem. Commun.* **2014**, *50*, 5455.
- (11) Cao, X.; Lin, W.; Yu, Q.; Wang, J. *Org. Lett.* **2011**, *13*, 6098.
- (12) Suzuki, S.; Kozaki, M.; Nozaki, K.; Okada, K. *J. Photochem. Photobiol. C: Photochem. Rev.* **2011**, *12*, 269.
- (13) Lin, H.-Y.; Huang, W.-C.; Chen, Y.-C.; Chou, H.-H.; Hsu, C.-Y.; Lin, J. T.; Lin, H.-W. *Chem. Commun.* **2012**, *48*, 8913.
- (14) Ooyama, Y.; Hagiwara, Y.; Mizumo, T.; Harima, Y.; Ohshita, J. *RSC Adv.* **2013**, *3*, 18099.
- (15) Kubota, Y.; Ozaki, Y.; Funabiki, K.; Matsui, M. *J. Org. Chem.* **2013**, *78*, 7058.

- 1
2
3
4
5
6
7
8
9
10
11
12
13
14
15
16
17
18
19
20
21
22
23
24
25
26
27
28
29
30
31
32
33
34
35
36
37
38
39
40
41
42
43
44
45
46
47
48
49
50
51
52
53
54
55
56
57
58
59
60
- (16) Kubota, Y.; Sakuma, Y.; Funabiki, K.; Matsui, M. *J. Phys. Chem. A* **2014**, *118*, 8717.
- (17) Kubota, Y.; Hara, H.; Tanaka, S.; Funabiki, K.; Matsui, M. *Org. Lett.* **2011**, *13*, 6544.
- (18) Graser, M.; Kopacka, H.; Wurst, K.; Ruetz, M.; Kreutz, C. R.; Müller, T.; Hirtenlehner, C.; Monkowius, U.; Knör, G.; Bildstein, B. *Inorg. Chim. Acta* **2013**, *405*, 116.
- (19) Xia, M.; Wu, B.; Xiang, G. *J. Fluor. Chem.* **2008**, *129*, 402.
- (20) Yan, W.; Wan, X.; Chen, Y. *J. Mol. Struct.* **2010**, *968*, 85.
- (21) Tokoro, Y.; Nagai, A.; Chujo, Y. *Macromolecules* **2010**, *43*, 6229.
- (22) Zhou, Y.; Xiao, Y.; Li, D.; Fu, M.; Qian, X. *J. Org. Chem.* **2008**, *73*, 1571.
- (23) Díaz-Moscoso, A.; Emond, E.; Hughes, D. L.; Tizzard, G. J.; Coles, S. J.; Cammidge, A. N. *J. Org. Chem.* **2014**, *79*, 8932.
- (24) Li, H.-J.; Fu, W.-F.; Li, L.; Gan, X.; Mu, W.-H.; Chen, W.-Q.; Duan, X.-M.; Song, H.-B. *Org. Lett.* **2010**, *12*, 2924.
- (25) Fischer, G. M.; Daltrozzi, E.; Zumbusch, A. *Angew. Chem. Int. Ed.* **2011**, *50*, 1406.
- (26) Nagai, A.; Kokado, K.; Nagata, Y.; Arita, M.; Chujo, Y. *J. Org. Chem.* **2008**, *73*, 8605.
- (27) Samonina-Kosicka, J.; DeRosa, C. A.; Morris, W. A.; Fan, Z.; Fraser, C. L. *Macromolecules* **2014**, *47*, 3736.
- (28) Poon, C.-T.; Lam, W. H.; Wong, H.-L.; Yam, V. W.-W. *J. Am. Chem. Soc.* **2010**, *132*, 13992.
- (29) Zhang, G.; St. Clair, T. L.; Fraser, C. L. *Macromolecules* **2009**, *42*, 3092.
- (30) Frath, D.; Azizi, S.; Ulrich, G.; Ziessel, R. *Org. Lett.* **2012**, *14*, 4774.
- (31) Frath, D.; Azizi, S. b.; Ulrich, G.; Retailleau, P.; Ziessel, R. *Org. Lett.* **2011**, *13*, 3414.
- (32) Yu, C.; Jiao, L.; Zhang, P.; Feng, Z.; Cheng, C.; Wei, Y.; Mu, X.; Hao, E. *Org. Lett.* **2014**, *16*, 3048.
- (33) Suresh, D.; Gomes, C. S. B.; Gomes, P. T.; Di Paolo, R. E.; Macanita, A. L.; Calhorda, M. J.; Charas, A.; Morgado, J.; Teresa Duarte, M. *J. Chem. Soc. Dalton. Trans.* **2012**, *41*, 8502.
- (34) Kertesz, M.; Choi, C. H.; Yang, S. *Chem. Rev.* **2005**, *105*, 3448.
- (35) Sobczyk, L.; Grabowski, S. J.; Krygowski, T. M. *Chem. Rev.* **2005**, *105*, 3513.
- (36) Raczyńska, E. D.; Kosińska, W.; Ośmiałowski, B.; Gawinecki, R. *Chem. Rev.* **2005**, *105*, 3561.
- (37) Cyrański, M. K. *Chem. Rev.* **2005**, *105*, 3773.
- (38) Ortí, E.; Viruela, R.; Viruela, P. M. *J. Phys. Chem.* **1996**, *100*, 6138.
- (39) Soldatova, A. V.; Kim, J.; Peng, X.; Rosa, A.; Ricciardi, G.; Kenney, M. E.; Rodgers, M. A. *J. Inorg. Chem.* **2007**, *46*, 2080.
- (40) Kolehmainen, E.; Ośmiałowski, B.; Krygowski, T. M.; Kauppinen, R.; Nissinen, M.; Gawinecki, R. *J. Chem. Soc. Perkin Trans. 2* **2000**, 1259.
- (41) Kolehmainen, E.; Ośmiałowski, B.; Nissinen, M.; Kauppinen, R.; Gawinecki, R. *J. Chem. Soc. Perkin Trans. 2* **2000**, 2185.
- (42) Ośmiałowski, B.; Kolehmainen, E.; Nissinen, M.; Krygowski, T. M.; Gawinecki, R. *J. Org. Chem.* **2002**, *67*, 3339.

- (43) Krygowski, T. M.; Zachara, J. E.; Ośmiałowski, B.; Gawinecki, R. *J. Org. Chem.* **2006**, *71*, 7678.
- (44) Min, J.; Ameri, T.; Gresser, R.; Lorenz-Rothe, M.; Baran, D.; Troeger, A.; Sgobba, V.; Leo, K.; Riede, M.; Guldi, D. M.; Brabec, C. J. *ACS Appl. Mater. Interfaces* **2013**, *5*, 5609.
- (45) Gresser, R.; Hummert, M.; Hartmann, H.; Leo, K.; Riede, M. *Chem. Eur. J.* **2011**, *17*, 2939.
- (46) Ni, Y.; Zeng, W.; Huang, K.-W.; Wu, J. *Chem. Commun.* **2013**, *49*, 1217.
- (47) Mueller, T.; Gresser, R.; Leo, K.; Riede, M. *Sol. Energ. Mat. Sol. C.* **2012**, *99*, 176.
- (48) Kubo, Y.; Minowa, Y.; Shoda, T.; Takeshita, K. *Tetrahedron Lett.* **2010**, *51*, 1600.
- (49) Zakrzewska, A.; Zaleśny, R.; Kolehmainen, E.; Ośmiałowski, B.; Jędrzejewska, B.; Ågren, H.; Pietrzak, M. *Dyes Pigments* **2013**, *99*, 957.
- (50) Yamaguchi, Y.; Matsubara, Y.; Ochi, T.; Wakamiya, T.; Yoshida, Z.-i. *J. Am. Chem. Soc.* **2008**, *130*, 13867.
- (51) Goldberg, N. N.; Barkley, L. B.; Levine, R. *J. Am. Chem. Soc.* **1951**, *73*, 4301.
- (52) Zakrzewska, A.; Kolehmainen, E.; Valkonen, A.; Haapaniemi, E.; Rissanen, K.; Chęcińska, L.; Ośmiałowski, B. *J. Phys. Chem. A* **2012**, *117*, 252.
- (53) Xu, S.; Evans, R. E.; Liu, T.; Zhang, G.; Demas, J. N.; Trindle, C. O.; Fraser, C. L. *Inorg. Chem.* **2013**, *52*, 3597.
- (54) Yu, Y.-H.; Descalzo, A. B.; Shen, Z.; Röhr, H.; Liu, Q.; Wang, Y.-W.; Spieles, M.; Li, Y.-Z.; Rurack, K.; You, X.-Z. *Chem.-Asian J.* **2006**, *1*, 176.
- (55) Hecht, M.; Fischer, T.; Dietrich, P.; Kraus, W.; Descalzo, A. B.; Unger, W. E. S.; Rurack, K. *ChemistryOpen* **2013**, *2*, 25.
- (56) Bura, T.; Retailleau, P.; Ulrich, G.; Ziessel, R. *J. Org. Chem.* **2011**, *76*, 1109.
- (57) Ono, M.; Watanabe, H.; Kimura, H.; Saji, H. *ACS Chem. Neurosci.* **2012**, *3*, 319.
- (58) Lager, E.; Liu, J.; Aguilar-Aguilar, A.; Tang, B. Z.; Peña-Cabrera, E. *J. Org. Chem.* **2009**, *74*, 2053.
- (59) Angulo, G.; Grampp, G.; Rosspeintner, A. *Spectrochim. Acta A* **2006**, *65*, 727.
- (60) Birks, J. B.; Dyson, D. J. *Proc. R. Soc. Lond. A* **1963**, *275*, 135.
- (61) Grabowski, Z. R.; Rotkiewicz, K.; Rettig, W. *Chem. Rev.* **2003**, *103*, 3899.
- (62) Wiggins, P.; Williams, J. A. G.; Tozer, D. J. *J. Chem. Phys.* **2009**, *131*, 091101.
- (63) Guido, C. A.; Mennucci, B.; Jacquemin, D.; Adamo, C. *Phys. Chem. Chem. Phys.* **2010**, *12*, 8016.
- (64) Barfield, M.; Fagerness, P. *J. Am. Chem. Soc.* **1997**, *119*, 8699.
- (65) Laurent, A. D.; Jacquemin, D. *Int. J. Quantum. Chem.* **2013**, *113*, 2019.
- (66) Jacquemin, D.; Perpète, E. A.; Ciofini, I.; Adamo, C.; Valero, R.; Zhao, Y.; Truhlar, D. G. *J. Chem. Theory Comput.* **2010**, *6*, 2071.
- (67) Silva-Junior, M. R.; Schreiber, M.; Sauer, S. P. A.; Thiel, W. *J. Chem. Phys.* **2008**, *129*, 104103.

- 1
2
3
4 (68) Chibani, S.; Le Guennic, B.; Charaf-Eddin, A.; Laurent, A. D.;
5 Jacquemin, D. *Chem. Sci.* **2013**, *4*, 1950.
6 (69) Le Guennic, B.; Chibani, S.; Charaf-Eddin, A.; Massue, J.; Ziessel, R.;
7 Ulrich, G.; Jacquemin, D. *Phys. Chem. Chem. Phys.* **2013**, *15*, 7534.
8 (70) Chibani, S.; Charaf-Eddin, A.; Le Guennic, B.; Jacquemin, D. *J. Chem.*
9 *Theory Comput.* **2013**, *9*, 3127.
10 (71) Er, J. C.; Tang, M. K.; Chia, C. G.; Liew, H.; Vendrell, M.; Chang, Y.-
11 T. *Chem. Sci.* **2013**, *4*, 2168.
12 (72) Jin, J.-L.; Li, H.-B.; Geng, Y.; Wu, Y.; Duan, Y.-A.; Su, Z.-M.
13 *ChemPhysChem* **2012**, *13*, 3714.
14 (73) Chibani, S.; Le Guennic, B.; Charaf-Eddin, A.; Maury, O.; Andraud,
15 C.; Jacquemin, D. *J. Chem. Theory Comput.* **2012**, *8*, 3303.
16 (74) Cammi, R.; Mennucci, B. *J. Chem. Phys.* **1999**, *110*, 9877.
17 (75) Chibani, S.; Budzak, S.; Medved, M.; Mennucci, B.; Jacquemin, D.
18 *Phys. Chem. Chem. Phys.* **2014**, *16*, 26024.
19 (76) Frisch, M. J.; Trucks, G. W.; Schlegel, H. B.; Scuseria, G. E.; Robb,
20 M. A.; Cheeseman, J. R.; Scalmani, G.; Barone, V.; Mennucci, B.; Petersson, G. A.;
21 Nakatsuji, H.; Caricato, M.; Li, X.; Hratchian, H. P.; Izmaylov, A. F.; Bloino, J.;
22 Zheng, G.; Sonnenberg, J. L.; Hada, M.; Ehara, M.; Toyota, K.; Fukuda, R.;
23 Hasegawa, J.; Ishida, M.; Nakajima, T.; Honda, Y.; Kitao, O.; Nakai, H.; Vreven, T.;
24 Montgomery, J., J. A. ; Peralta, J. E.; Ogliaro, F.; Bearpark, M.; Heyd, J. J.; Brothers,
25 E.; Kudin, K. N.; Staroverov, V. N.; Kobayashi, R.; Normand, J.; Raghavachari, K.;
26 Rendell, A.; Burant, J. C.; Iyengar, S. S.; Tomasi, J.; Cossi, M.; Rega, N.; Millam, J.
27 M.; Klene, M.; Knox, J. E.; Cross, J. B.; Bakken, V.; Adamo, C.; Jaramillo, J.;
28 Gomperts, R.; Stratmann, R. E.; Yazyev, O.; Austin, A. J.; Cammi, R.; Pomelli, C.;
29 Ochterski, J. W.; Martin, R. L.; Morokuma, K.; Zakrzewski, V. G.; Voth, G. A.;
30 Salvador, P.; Dannenberg, J. J.; Dapprich, S.; Daniels, A. D.; Farkas, O.; Foresman, J.
31 B.; Ortiz, J. V.; Cioslowski, J.; Fox, D. J. In *Gaussian 09, Revision A.02*; Gaussian,
32 Inc.: Wallingford CT, 2009.
33 (77) Petrenko, T.; Neese, F. *J. Chem. Phys.* **2007**, *127*, 164319.
34 (78) Savarese, M.; Aliberti, A.; De Santo, I.; Battista, E.; Causa, F.; Netti,
35 P. A.; Rega, N. *J. Phys. Chem. A* **2012**, *116*, 7491.
36
37
38
39
40
41
42
43
44
45
46
47
48
49
50
51
52
53
54
55
56
57
58
59
60